Phys. Status Solidi C **7**, No. 3–4, 852–856 (2010) / **DOI** 10.1002/pssc.200982694

physica status solidi c
www.pss-c.com
current topics in solid state physics

Investigation of defect states in the amorphous phase of phase change alloys GeTe and $Ge_2Sb_2Te_5$

Jennifer Luckas[*,1], Daniel Krebs[1], Martin Salinga[1], Matthias Wuttig[1], and Christophe Longeaud[2]

[1] RWTH Aachen University, I. Physikalisches Institut (IA), 52056 Aachen, Germany
[2] Laboratoire de Génie Electrique de Paris (CNRS UMR 8507), Plateau de Moulon, 11 rue Joliot Curie, 91190 Gif sur Yvette, France

Received 27 July 2009, revised 7 October 2009, accepted 15 October 2009
Published online 19 January 2010

PACS 61.43.Dq, 71.23.Cq, 71.55.Jv, 72.40.+w

* Corresponding author: e-mail jennifer.luckas@physik.rwth-aachen.de, Phone: + 49 241 80 27175, Fax:+ 49 241 80 22331

In amorphous materials localized states within the band gap govern the electronic transport properties. This work presents the first measurement of the density of states within the band gap of amorphous phase change alloys using modulated photo current experiments. Modulated photo current measurements performed on a-$Ge_{50}Te_{50}$ and a-$Ge_2Sb_2Te_5$ show that the defect state density of both compositions is quite similar consisting of a pronounced valence band tail and at least two defect states.

1 Introduction Chalcogenide-based phase change alloys combine many exceptional properties [1]. Firstly, they show a temperature induced phase transition between the amorphous and the crystalline state that can proceed on the nano second time scale at elevated temperatures. Secondly, the optical and electrical properties of the amorphous and crystalline structure differ drastically [2]. Additionally, phase change materials enable an enormous scalability down to a few nanometres [3]. This extraordinary combination of properties makes phase change alloys promising candidates for a non-volatile electronic data storage technology [4]. To advance this storage concept, the charge transport in the amorphous and crystalline state has to be understood and the electronic switching mechanism [5] needs to be unravelled.

Localized states within the band gap can arise from the lack of long range order and thus constitute an intrinsic property of disordered material. They strongly influence the electronic transport properties. For instance they play a dominant role in defining the position of the Fermi level within the band gap.

In the 1970's the Valence alternation Pair band model was suggested for amorphous chalcogenides [7,8]. This model is based on chemical-bonding arrangements. Due to the 8-N rule, chalcogenides exhibit divalent bonding denoted as C_2^0 centre, where C stands for chalcogen, the subscript 2 gives the covalent coordination and the superscript 0 the charge state. The expected existence of one dimensional Te-Te chains gives rise to a high concentration of electrons, that do not participate in ordinary covalent bonding. These electrons form so-called lone pairs, which have a wide spectrum of orientations in the amorphous phase inducing a pronounced band tail of the valence band. Breaking bonds along the Te-Te chain causes so-called valence-alternation pairs (VAPs): a three-fold coordinated, positively charged C_3^+ defect and a negatively charged, one fold coordinated C_1^- defect [7]. These defects create a donor-like and an acceptor-like imperfection band pinning the Fermi energy E_F in the middle of the mobility band gap [8].

In recent years a model for the switching mechanism has been developed [6], which assumes a certain number of defects in the amorphous phase according to the

VAP model. A detailed experimental study of these defects is still missing however.
Furthermore, recent structural analysis performed on amorphous $Ge_2Sb_2Te_5$ show that Te-Te bonds are only rarely realized, which one study finds on average 0.288 Te atoms as nearest neighbours of a Te atom [9] and several other studies find no such pairs at all [10-12]. Since the existence of Te-Te chains in amorphous Ge-Sb-Te alloys could not be unambiguously verified, the validity of the theoretical VAP band model consisting of a pronounced valence band and a donor/acceptor pair is questionable. Therefore the development of a new model is indispensable, that takes into account the recent structure determination of the amorphous state. To develop such a model the defect state density within the band gap has been probed by modulated photocurrent measurements.

2 Modulated photo current (MPC) – experimental procedure The MPC sample consists of a thin film of thickness d of the material under investigation on an electrically insulating substrate. On top of the film there are two parallel electrodes of length l, so that a dc voltage can be applied to the rectangular area of the material under investigation between them. A light source illuminating the sample surface is amplitude-modulated with angular frequency ω. This way a modulated photo current is induced within the conduction cross section $A=d\cdot l$ due to band to band excitation. The generated photo carriers propagating with free carrier mobility μ are captured by localized states within the band gap. The higher the value for the capture coefficient c, the stronger is this interaction. As long as hopping conduction can be neglected trapped carriers do not contribute to the photo current. After a certain time a trapped carrier is thermally released back to extended states above the mobility band edge contributing to photo conductivity again. As a consequence of these multiple trapping and release processes the modulated photo current lags in general behind the modulated excitation resulting in a positive phase shift ϕ. The phase shift ϕ and the amplitude of the alternating part of the photocurrent I_{ac} are measured with a lock-in-amplifier. Based on the rate equations determining the free and trapped carrier concentrations the density of states within the band gap $N(E)$ can be related to the measured quantities ϕ and I_{ac} under the assumptions that multiple trapping processes exceed recombination and the photocurrent is mainly driven by one type of carriers [13-15]. One has:

$$\frac{cN(E_\omega)}{\mu} = \frac{2}{\pi}\frac{Aq\varepsilon G_{ac}\sin(\phi)}{|I_{ac}|}, \qquad (1)$$

where ε is the applied electric field, q is the absolute value of the electronic charge and G_{ac} the ac generation rate. If holes are majority carriers, the probed states are located at an energy E_ω above the valence band edge E_v given by:

$$E_\omega = E - E_v = k_b T \ln(\nu_p/\omega), \qquad (2)$$

where k_b is the Boltzmann constant and ν_p the attempt-to-escape frequency for holes. The latter equals the product of the capture coefficient c_p and the equivalent density at the valence band edge N_v. If the photocurrent is dominated by electrons E_ω is given by the energetic distance of the probed gap state to the mobility edge of the conduction band and ν_p has to be replaced by ν_n, the attempt to escape frequency for electrons. The attempt-to-escape frequency can not be measured directly, but can be obtained from the analysis of MPC data.
According to Eq. (1) and (2) the spectroscopy of the relative density of states within the band gap $cN(E)/\mu$ is possible by measuring couples (ϕ, I_{ac}) at different excitation frequencies ω and temperatures T. At first sight it seems that the measurement range of MPC is only limited by the experimentally accessible conditions of ω and T, since even a deep state in the gap could be probed using adequate high temperatures and low excitation frequencies. However, it has to be remembered that Eq. (1) and (2) are only valid for gap states acting as multiple trapping centres.
On the contrary a carrier captured by gap states lying energetically deep within the mobility band gap will more likely recombine than being thermally released back to the band from which it has been captured. Thus recombination centres are energetically located near the Fermi energy E_F. The width of this recombination region decreases with increasing intensity of the excitation light and decreasing temperature [16]. In consequence the analysis of MPC data via Eq. (1) and (2) enables at most the investigation of the gap state density from one mobility band edge to the Fermi energy, but not within the whole band gap.

3 Pre-experiments

3.1 Sample preparation On a glass substrate (thickness: 0.5-0.6 mm) a phase change films (d = 100 nm or 500 nm) and two parallel rectangular Al electrodes (8mm x 2mm x 100 nm) 1.5 mm apart along their long side were deposited successively by dc sputtering.

3.2 Dark conductivity Temperature dependent measurements of the dark conductivity were performed in a cryostat from room temperature down to 100 K and vice versa in either 10 K or 5 K steps under vacuum conditions (~10^{-5} Torr). By applying a dc voltage to the electrodes the dark current at the set temperature value T is measured ten times in a row. The results of these ten measurements are averaged to determine the dark conductivity at temperature T. The results of these measurements are plotted in Fig. 1 assuming a thermally activated transport described by an Arrhenius behaviour.

$$\sigma_{dark} = C\exp(-E_a/k_bT), \qquad (3)$$

where the activation energy E_a defines the slope in the Arrhenius-plot. From Fig. 1 it can be clearly seen that neither a-$Ge_{50}Te_{50}$ nor a-$Ge_2Sb_2Te_5$ can be properly described by a single activation energy E_a over the whole temperature range. However at high temperatures, i.e. from 200 K to 300 K, the Arrhenius plot gives a straight line revealing an activation energy E_a=0.34 eV and C=228 S/cm for a-$Ge_{50}Te_{50}$ and E_a=0.36 eV and C=647 S/cm for a-$Ge_2Sb_2Te_5$. The same data are plotted in Fig. 2 using Mott's law [17]

$$\sigma_{dark} = A\exp\left[-(T_0/T)^{1/4}\right], \quad (4)$$

Though a matter of controversy [21], Mott's law implies variable range hopping conduction in the vicinity of the Fermi level with a constant density of states $N(E_F)$. The characteristic temperature T_0 is given by:

$$T_0 = \beta / k_b N(E_F)\alpha^3 \quad (5)$$

Various theoretical studies in three-dimensional systems suggest β values in the range from 10.0 to 37.8 [20]. The parameter α describes the extension of the localized wave function. In this work α is assumed to be α=2·10^{-7} cm to estimate the order of magnitude of the density of states at the Fermi energy $N(E_F)$ from the characteristic temperature T_0. While a-$Ge_{50}Te_{50}$ can be properly described by Mott's law only in a limited temperature range between 100 K and 170 K, a-$Ge_2Sb_2Te_5$ shows a good agreement over the whole investigated temperature range. The characteristic temperature was derived from Fig. 2 to be $T_0^{1/4}$=157 $K^{1/4}$ for a-$Ge_{50}Te_{50}$ and $T_0^{1/4}$=191 $K^{1/4}$ for a-$Ge_2Sb_2Te_5$. Consequently the density of states at the Fermi energy is of the order $N(E_F)$~10^{16} $eV^{-1}cm^{-3}$ for both phase change alloys.

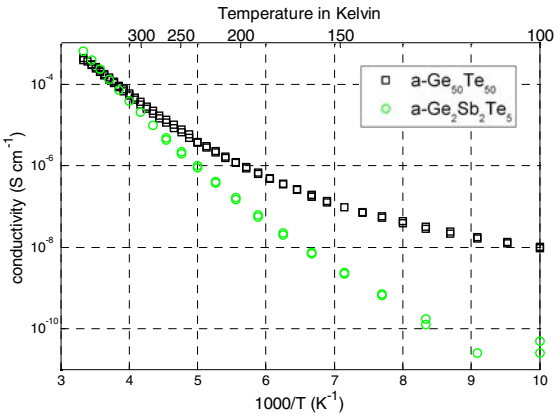

Figure 1 Temperature dependence of the dark conductivity measured on a-$Ge_{50}Te_{50}$ and a-$Ge_2Sb_2Te_5$ samples.

3.3 Photoconductivity To measure the photoconductivity the sample was illuminated with a constant light flux F_{cw}=$10^{16}cm^{-2}s^{-1}$ at the wavelength λ=850 nm. These measurements were directly performed after a measurement of the dark current at each temperature T. To ensure steady state conditions the sample was illuminated one minute, before the current, consisting of photo and dark current

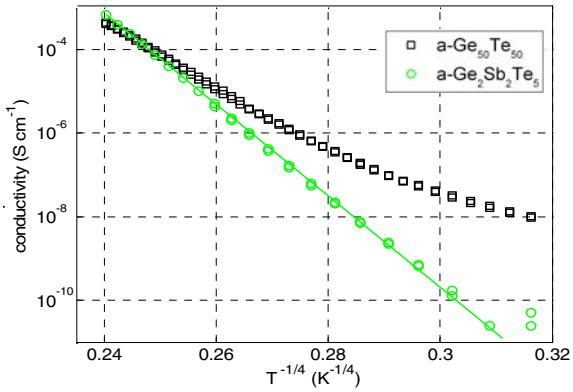

Figure 2 Plot of the dark conductivity applying Mott law to the same data as in Fig 1 for both samples.

was measured. The photocurrent was given by the difference of the measured current and the dark current. The results obtained for a-$Ge_{50}Te_{50}$ and a-$Ge_2Sb_2Te_5$ are presented in Fig. 3. The general behaviour observed for a-$Ge_2Sb_2Te_5$ agrees with what is reported in the literature [18]. The continuous decrease measured on both materials at high temperatures could be a consequence of measurement errors, since at high temperatures the current and the dark current do not differ much.

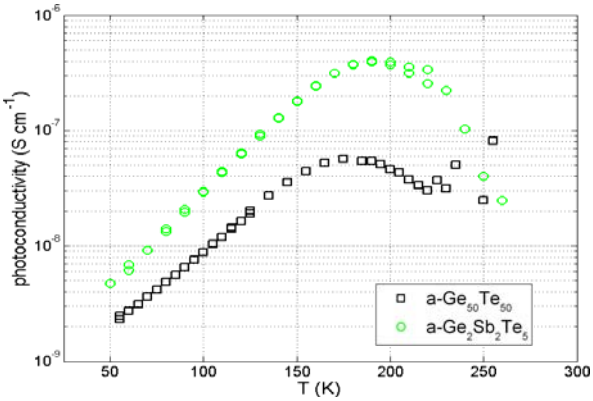

Figure 3 Temperature dependence of the photoconductivity measured on 100 nm thick chalcogenide samples.

4 MPC - results Since chalcogenides are known to be p-type conducting in dark equilibrium we assume that the photo current is also mainly driven by holes. MPC measurements were performed in the same cryostat as the conductivity measurements using a wavelength of λ=850 nm and a continuous photon flux F_{cw}=$10^{16}cm^{-2}s^{-1}$. The amplitude of the alternating photon flux was chosen to be 40% of the continuous flux. At a given temperature T the data points were obtained varying the excitation frequency $f=\omega/2\pi$ in a range from 12 Hz to 40 kHz in a way such that $f_{i+1}=f_i$ x 1.5. The results are shown in Fig. 4. Each data set corresponds to a certain temperature. Within the data set, energy states closer to the valence band edge were probed

with 40 kHz while the energy states located furthest away from the band edge were sampled with 12 Hz, see Eq. (1) and Eq. (2). The temperature steps have to be chosen sufficiently small, since only the envelope of the superimposing MPC curves reveals the relative density of states $cN(E)/\mu$. The temperature steps were chosen to be at the most 20 K and sometimes even as low as 5 K to obtain a good resolution of the density of states.

Until now there is no experiment to determine the attempt-to-escape-frequency ν. Thus we have to assume a value that defines the energy scaling of the MPC data. If a wrong attempt-to-escape frequency ν is chosen, the MPC curves, obtained at different temperatures T, do not superimpose according to Eq. (2). The energy scaling was performed assuming an equivalent density of the valence band as observed in amorphous silicon of $N_v = 2.5 \cdot 10^{19} \mathrm{cm}^{-3}$.

Both MPC spectra obtained for a-$Ge_{50}Te_{50}$ and a-$Ge_2Sb_2Te_5$ reveal a band tail and two defect peaks. The band tail and the defect peak probed at 300 K are scaled using $\nu = c \cdot N_v = 10^{12} \mathrm{s}^{-1}$, i.e. $c = 4 \cdot 10^{-8} \mathrm{cm}^3 \mathrm{s}^{-1}$. This choice of ν describes properly the probed band tail states, since the MPC curves measured at different temperatures superimpose quite well at least at high frequencies. In the low frequency range we observe almost parallel lines, the shape of which is unchanged by a reduction of the dc flux by a factor of five. Hence, these parallel lines are a fingerprint in the MPC spectra of active hopping processes at these low temperatures [17]. The defect peak observed around 240 K in contrast is best described assuming $\nu = 2.5 \cdot 10^{8} \mathrm{s}^{-1}$, i.e. $c = 10^{-11} \mathrm{cm}^3 \mathrm{s}^{-1}$.

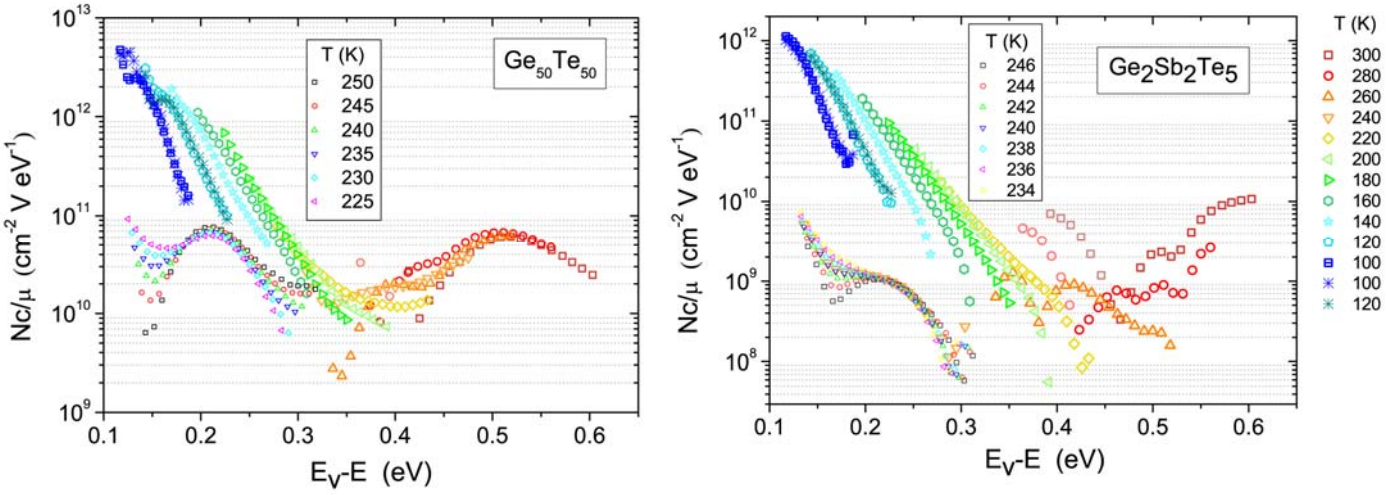

Figure 4 The MPC-spectra obtained on a-$Ge_{50}Te_{50}$ (left) and a-$Ge_2Sb_2Te_5$ (right) samples reveal a band tail and a defect peak scaled assuming an attempt to escape frequency $\nu = 10^{12}\ \mathrm{s}^{-1}$ (large symbols). A second defect peak that scales with $\nu = 2.5 \cdot 10^{-8} \mathrm{s}^{-1}$ is probed around 240 K (small symbols). The MPC curves obtained at low temperatures were measured once more using a dc flux reduced by a factor 5 (asterisks).

5 Conclusion The MPC spectra obtained on a-$Ge_{50}Te_{50}$ and a- $Ge_2Sb_2Te_5$ are quite similar for both compositions revealing a band tail and two defect states. However, compared to a- $Ge_{50}Te_{50}$ a-$Ge_2Sb_2Te_5$ possesses a lower relative defect density Nc/μ explaining its higher photo conductivity. At high temperatures the photoconductivity is mostly influenced by the deep defect having a large capture coefficient c, since both quantities differ by the same factor. For both alloys an Arrhenius behaviour of the dark conductivity is observed in a small temperature range from 200 K to 300 K. The corresponding activation energy E_a agrees with the energetic position of the two defect peaks.

Acknowledgements We thank our colleagues Michael Woda and Michael Klein for the sample preparation and the Deutscher Akademischer Austausch Dienst (DAAD) for financial support.

References

[1] M. Wuttig and N. Yamada, Nature Mater. **6**, 824 (2007).
[2] K. Shportko, S. Kremers, M. Woda, D. Lencer, J. Robertson, and M. Wuttig, Nature Mater. **7**, 653 (2008).
[3] S. Raux et al., Microelectron. Eng. **85**, 2330-2333 (2008).
[4] S.R. Ovshinsky, Phys. Rev. Lett. **21**, 1450 (1968).
[5] D. Adler, Amorphous Semiconductors (The Butterworth Group, 1971).
[6] A. Pirovano et al., IEEE Trans. Electron. Devices **51**, 452 - 459 (2004).
[7] M. Kastner, D. Adler, and H. Fritzsche, Phys. Rev. Lett. **37**, 1504-1507 (1976).

[8] S.R. Ovshinsky and D. Adler, Contemp. Phys. **19**, 109-126 (1978).
[9] S. Caravati et al., Appl. Phys. Lett. **91**, 171906 (2007).
[10] J. Akola and R. O. Jones, Phys. Rev. B **76**, 235201 (2007).
[11] P. Jovari et al., Phys. Rev. B **77**, 035202 (2008).
[12] S. Kohara et al., Appl. Phys. Lett. **89**, 201910 (2006).
[13] H. Oheda, J. Appl. Phys. **52**, 6693-6700 (1981).
[14] R. Brüggemann, C. Main, J. Berkin, and S. Reynolds, Philos. Mag. B **62**, 29-45 (1990).
[15] C. Longeaud and J.P. Kleider, Phys. Rev. B **45**, 11672-11684 (1980).
[16] W. Shockley and W.T. Read, Phys. Rev. B **87**, 835-842 (1952).
[17] N.F. Mott and E.A. Davis (eds.), Electronic processes in non-crystalline solids (Clarendron Press Oxford, 1971).
[18] W. Howard and R. Tsu, Phys. Rev. **1**, 4709-4719 (1952).
[19] C. Longeaud and S. Tobbeche, J. Phys.: Condens. Matter **21,** 4709-4719 (2009).
[20] C. H. Seager and G.E. Pike, Phys. Rev. B **10**, 1435 (1974).
[21] J. M. Marshall and C. Main, J. Phys.: Condens. Matter **20**, 285210 (2008).

